NANOSYSTEMS: PHYSICS, CHEMISTRY, MATHEMATICS, 2014, 5 (1), P. 53–61

FULLERENE FILMS WITH SUPPRESSED POLYMERIZING ABILITY

M. Yesilbas[1*], T. L. Makarova[1,2], I. Zakharova[3]

[1]Umeå University, 90187 Umeå, Sweden

[2]Ioffe Physico-technical Institute, 194021 St. Petersburg, Russia

[3]State Technical University, 195251 St. Petersburg, Russia

*merveyesilbas.my@gmail.com

PACS 61.48.+c

Illumination of fullerene with visible light in the presence of oxygen leads to a transition of oxygen from triplet (ground) to singlet (excited) state where singlet oxygen is a long-lived reactive oxygen species. The effectiveness of fullerene as a singlet oxygen generator drastically decreases when fullerenes are condensed into a bulk material, mainly due to the polymerization ability. The ability of fullerene films to polymerize was studied for the C_{60} fullerene films intercalated with tetraphenylporphyrine (TPP), CdS, CdTe, HNO_3 as well as the hydrogen plasma treated films. Raman spectroscopy was used for monitoring the polymerization process. The ability to polymerize was found to be tightly connected to the formation of charge-transfer (Wannier-Mott) excitons which are revealed in the absorption spectra and measured with the help of spectroscopic ellipsometry.

Keywords: Fullerene, CdS, CdTe, HNO_3, tetraphenylporphyrine, hydrogen plasma, Raman spectroscopy, spectroscopic ellipsometry, polymerization.

1. Introduction

Molecular oxygen also known as dioxygen (O_2) is a powerful oxidant which can destroy organic compounds quickly. Dioxygen in its ground state is present in triplet form ($^3O_2$) which has a total spin of unity (S=1). Singlet oxygen ($^1O_2$) is a long-lived reactive oxygen species resulting from spin-forbidden transition from the ground state to the excited state of O_2 where the total spin is zero (S=0), thus and providing its very reactive behavior [1, 2]. Highly efficient production of $^1O_2$ proceeds in the presence of a photosensitizer dye by low-energy illumination. In the liquid phase, there have been many applications of singlet oxygen, however, in the gas phase the utilization of $^1O_2$ has been unexplored due to technical problems with the light stability of the photosensitizers. In particular, fullerenes promote the transition of molecular oxygen from a triplet to a singlet state in case of irradiation with visible light [1, 3] and this compound is then used to inactivate the viruses and bacteria [4-6], especially common in photodynamic therapy (PDT) [7, 8]. The effectiveness of fullerene molecules as photosensitizers is limited by their ability to form polymeric structures.

Fullerene (C_{60}) presents the f.c.c. structure with weak Van der Waals intermolecular bonds and can be transformed into different polymeric structures. The polymerization leads to a change in the structural, mechanical and electrical properties of pristine form of the C_{60} [9]. Fullerenes can be polymerized in three different ways: photopolymerization, pressure polymerization and intercalation of C_{60} structure with a guest compound [10]. In this work, the photopolymerization method was used, irradiating the thin C_{60} films with visible light. In the so-called [2+2] cycloaddition, some of the double bonds on the molecule break up and linked to an adjacent molecule forming a 'cyclobutane ring' that consists four carbon atoms

[9]. In the cycloaddition process, double bonds of adjacent molecules are oriented parallel and complete polymerization then leads to a decrease in the distance between the molecules to 9.1–9.2 Å from the value of 10 Å in the case of unpolymerized state [11, 12]. The creation of intermolecular bonds stops the rotation of molecule and lowers the symmetry, which can be detected in Raman spectroscopy. The high icosahedral (I_h) symmetry with a high Raman scattering cross section of C_{60} enables Raman spectroscopy to be a very efficient tool for monitoring the polymerization. The formation of new bonds changes the mode positions of molecular vibrations, especially in $A_g(2)$ also called 'pentagonal pinch mode' [9, 13]. There are several factors affecting the position of the $A_g(2)$ mode, including polymerization and charge transfer. The calculations of *Porezag et.al.* [14] show that the $A_g(2)$ mode, which is situated at 1469 cm^{-1} in pristine C_{60}, should be linearly downshifted due to the number of polymer bonds, which was confirmed experimentally [15]. The calculated $A_g(2)$ mode position for the different phases of C_{60} due to calculation is shown in table 1.

TABLE 1. Shifted positions of the A_g (2) - derived mode for different phases of C_{60}[1]

Phase	Number of polymer bonds	$A_g(2)$ mode position (cm^{-1})
Pristine	0	1469
Dimers	1	1464
Orthorhombic	2	1459
Branched chains	3	1454
Tetragonal	4	1448
Rhombohedral	6	1407

[1]Reference [9]

In the bulk form of C_{60}, an inter-molecular type of exciton exists which is also called the charge-transfer (CT) exciton. The formation of CT-excitons is a precursor to photopolymerization. The probability of exciton formation decreases when the guest molecules are intercalated in the voids of crystalline lattice in fullerene solids. Another way of preventing polymerization is the functionalization of fullerene molecules. The polymerization process on C_{60} is illustrated in figure 1 where two hexagon bonds of the fullerene are presented as 'active sites (6=6)'. In the figure 1, the polymerization of pristine C_{60} in upper and hydrogen plasma treatment C_{60} in lower part is presented. The figure 1 shows that hydrogen plasma treatment of C_{60} protects the active sites (6=6) and thus prevents polymerization.

In this work, the polymerization process was monitored by Raman spectroscopy. Simultaneously, the formation of the CT- excitons in the C_{60} was exctracted from the absorption spectra measured by the spectroscopic ellipsometry.

2. Experimental Part

2.1. Methods of Production of Films

C_{60} films were produced by using a quasi-closed volume vacuum evaporation technique. Films were prepared by discrete evaporation in a quasi-closed volume under a vacuum chamber pressure of 10^{-7} Torr. The semiconducting fullerene films were grown on glass substrates/ITO and silicon substrate. Then, the films were coevaporated with cadmium sulfide (CdS), cadmium telluride (CdTe), nitric acid (HNO_3) and tetraphenylporphyrin (TPP or H_2TPP) or treated in the hydrogen plasma discharge (C_{60}:H). The synthetic parameters for the films are given in table 2.

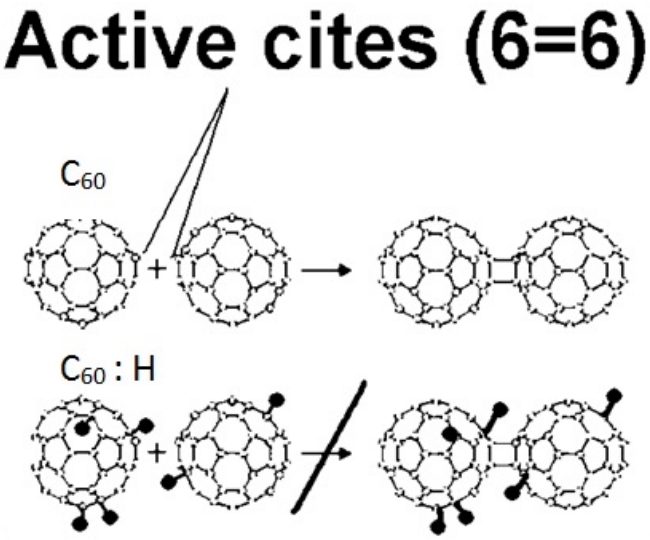

FIG. 1. Polymerization ability for C_{60} (upper) and hydrogenated C_{60} (lower)

TABLE 2. The synthetic parameters for C_{60} films

Film #	Content	Composition ratio	$T_{evaporator}$, C	$T_{substrate}$, C	Deposition time, min
111	$C_{60}HNO_3$	-	500	130	10
113	$C_{60}HNO_3$	-	500	130	5
114[2]	C_{60}	-	510	200	12
149	C_{60}:CdS	1:1	560	240	4
151	C_{60}:CdS	1:3	520	210	3
154	C_{60}:CdS	1:10	520	215	4
02_69	H_2TPP	-	320	150	5

[2] The sample was exposed to hydrogen plasma after the coevaporation

In hydrogen plasma treatment, the plasma chemical reactor, which is formed by a d.c. diode system with tungsten electrodes, was used operating a current density of less than 0.3 A/cm^2. The treatment was done at very low H pressure (p = 3–10 kP) and the films were on the periphery of the plasma discharge. The aim of producing hydrogen plasma treatment films in this experiment is to produce samples with very low concentration of hydrogen which means the hydrogen amount on attached fullerene is as small as possible and reducing pressure any more could lead to a quenching of the discharge.

2.2. Characterization of Films

A single grating Raman spectrometer (Renishaw 1000 Raman system) equipped with the three different lasers (514, 633 and 875 nm) and a CCD-detector was used for probing the polymerization. Measurements were performed at a wavelength of 514 nm with output power 1.8 mW. Scanning was done using an Olympus microscope attachment with 50x objective and the diameter of the focal spot approx 5 mkm. Filters were used to reduce the performance to 10% and 1%, and the spectral data were independent of the laser power. The device collects the information from the central spot of 1 micrometer diameter. Taking into account that the laser operates on a fundamental transverse mode and emits a beam

that approximates a Gaussian profile, we estimate the power density in the central 1-μm spot at 10% laser intensity as 0.3 mW/mm^2. As a general rule, dimer formation requires the absorption of one photon in photo-induced polymerization of C_{60} and a preferred range of fluences is 1 mW/mm^2 to 1000 mW/mm^2. A similar range of fluences can also be used for photo-assisted oxygen doping [16,17]. The spectral range for the films was determined from 200–1800 cm^{-1} for 1^{st} order, while the 2^{nd} order spectra of the hydrogen plasma-treated films were probed from 2000–4000 cm^{-1}. The spectroscopic data for CT-excitons were obtained by rotating analyzer ellipsometer (J. A. Woollam Co., Inc. Ellipsometry Solutions, α- SE^{TM}) which provided the spectral range between 380 nm to 900 nm. Ellipsometry presents an indirect technique which requires an evaluated fix optical modeling with the experimental data. In our case, the semiconductor films presents the four- layer thickness where a layer of fullerene lies on the silicon substrate which has a native oxide and surface roughness. In turn, fullerene also has a surface layer with a certain roughness which effects the light reflection. The surface roughness value was measured by an Atomic Force Microscope and a value between 15–20 nm was obtained for several samples. Our films were modeled as a 3-layer thickness using EMA (Bruggeman Effective Medium Approximation) model.

3. Results and Discussions

3.1. Raman Spectroscopy

The A_g (2) mode presents a fingerprint property for the polymerization process and is downshifted due to the number of polymer bonds occurring, as was previously mentioned in [17]. The peaks in the A_g (2) mode region were fitted by Voigt lineshape using a program named (PeakFitTM program, Version 4 for Win32). The A_g (2) mode is a non-degenerate peak that cannot split. The appearance of the satellite presents the A_g (2) derived modes which means the film polymerizes (Fig.2).

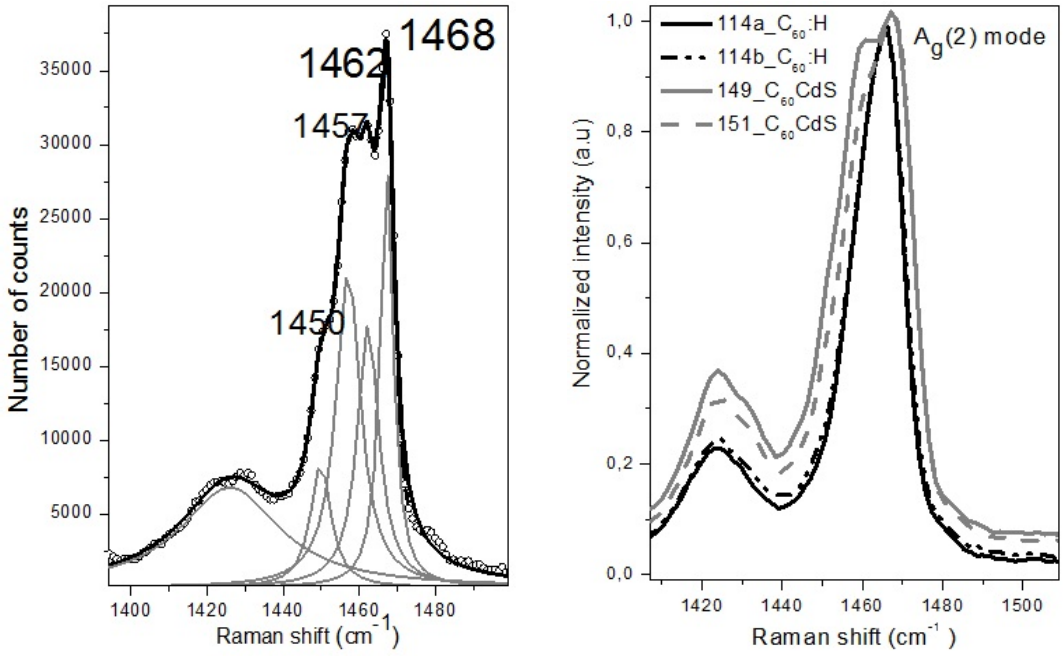

a) b)

FIG. 2. A_g (2) modes (a) pristine C_{60}, (b) hydrogen treatment and CdS intercalated films

In panel 1, comparison of A_g (2) modes for pristine C_{60} in (a), hydrogen-treated and CdS intercalated films in (b) are presented.

Pristine C_{60} presents a peak at 1468 cm^{-1}, as well as A_g-derived modes at the positions of 1462, 1457 $cm^{-1}$and 1450 cm^{-1}, corresponding to dimers and linear chains, and even the signs of two-dimensional polymerization respectively. The spectra in Fig. 2 (a) show that pristine C_{60} strongly polymerizes under the laser light. In Fig.2 (b), CdS intercalated and hydrogen treatment films presents less polymerized structure. Especially, hydrogen plasma treatment films serve the narrowest peaks in the vicinity of A_g (2) mode. It can be concluded that hydrogen plasma treatment films provides the best results for preventing polymerization.

In our experiments, TPP and HNO_3 intercalated films showed the most split structure in the vicinity of the A_g (2) mode region (Fig. 3). We believe, that in this case, the splitting is related to charge transfer processes between the fullerene matrix and the guest molecules.

Having found that hydrogenated films are the most resistant to polymerization, we further studied the aging effects and compared the spectra of freshly prepared hydrogenated films with the ones kept over 4 years under ambient conditions.

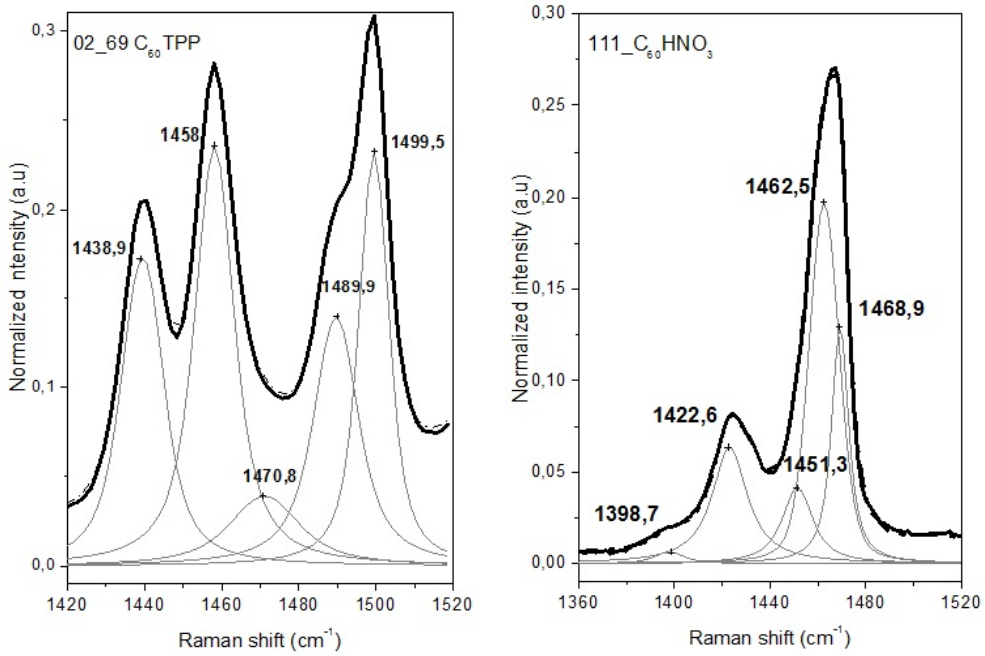

a) b)

FIG. 3. A_g (2) mode positions of TPP and HNO_3 intercalated films

The aging effects on the hydrogenated films in the 1^{st} and 2^{nd} order spectra were monitored by Raman spectroscopy. In the 1^{st} order spectra shown in figure 4, the pristine C_{60} film presents an unpolymerized peak at 1469 cm^{-1} and a derived mode at 1461 cm^{-1}. The freshly hydrogenated plasma treated film shows one unpolymerized peak at 1469 cm^{-1} but the aged hydrogenated film (2012) shows two peaks at 1463 and 1469 cm^{-1} mode positions where the area of first peak is twice as large as the second one. It can be concluded that the ability to polymerize has been restored.

To further analyze the aging effects, the 2^{nd} order spectra of the hydrogenated plasma treated films were probed. Although pristine C_{60} has no spectral features in the 1800–4000 cm^{-1} region, hydrogen plasma treatment of C_{60} reveals its sleeping modes and enables

a rich spectrum. The observation of the second order spectra of the fullerene films is a phenomenon which requires the absence of a polymerized phase and can be reached by either cooling below the glass transition temperature or heating above 450 K; also strong laser intensity is required [18].

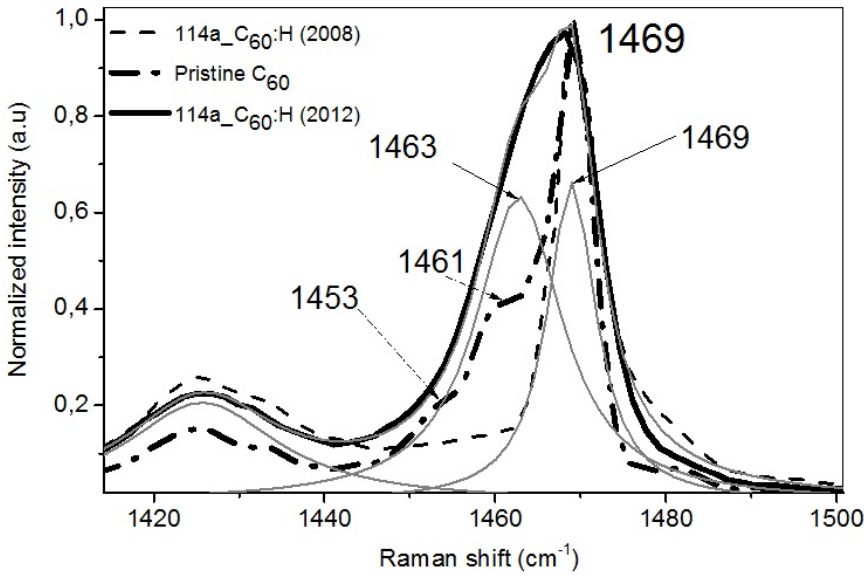

FIG. 4. Ageing effect on hydrogenated films[3] in the vicinity of Ag (2) mode position

We were especially interested in the 2800–3000 cm^{-1} spectral region, which is where C-H stretching vibrations are found, is also where the second order peaks interfere. We used a very low intensity laser (1.8 mW) at room temperature in our experiments. Figure 5 demonstrates that the spectral features in the 2800–3000 cm^{-1} region are much stronger than in other regions depending on C-H stretching vibrations.

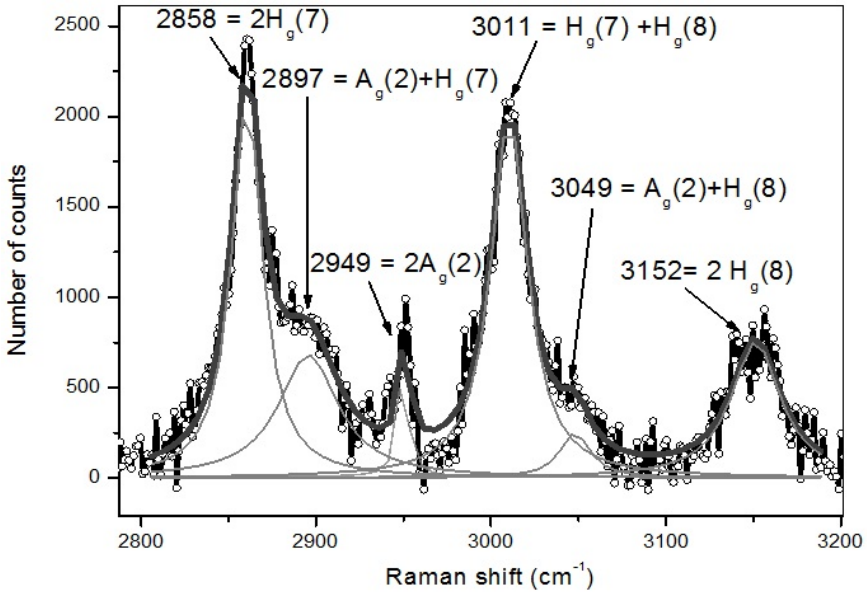

FIG. 5. The spectral region in 2800–3000 cm^{-1} for C_{60}:H (2008) film. This region is also reported as C-H stretching vibrations for $C_{60}H_{36}$ [16]

Additionally, spectral features have been preserved in samples aged for four years in this region only. As a final discussion, plasma treated samples presented the best results for suppression of the ability to polymerize when hydrogen was attached to the active sites of fullerene, the so-called 6=6 bonds. The absence of polymerization leads to the generation of a large number of second order peaks in the Raman spectra, which was confirmed and expressed in detail by Dong [18]. The plasma treated films were unstable, except in the C-H stretching region from 2800–3000 cm^{-1}.

3.2. Spectroscopic Ellipsometry

CT- excitons revealed in absorption spectra were measured with ellipsometry. The spectral features of the films were probed by comparison of the experimental and theoretical data. In the ellipsometry analysis, the films were modeled as a trilayer including a surface roughness of 200 Å. The ellipsometric model was constructed using both experimental and calculated data from the program and the spectra from which the film's absorption coefficients were determined. Using the measured Ψ and Δ ellipsometric parameters, an extinction coefficient was obtained and then the absorption coefficient was calculated by equation (1):

$$\alpha = \frac{4\pi k}{\lambda} \quad , \tag{1}$$

where k is the extinction coefficient of the films. The results for the absorption coefficients are given in Figure 6.

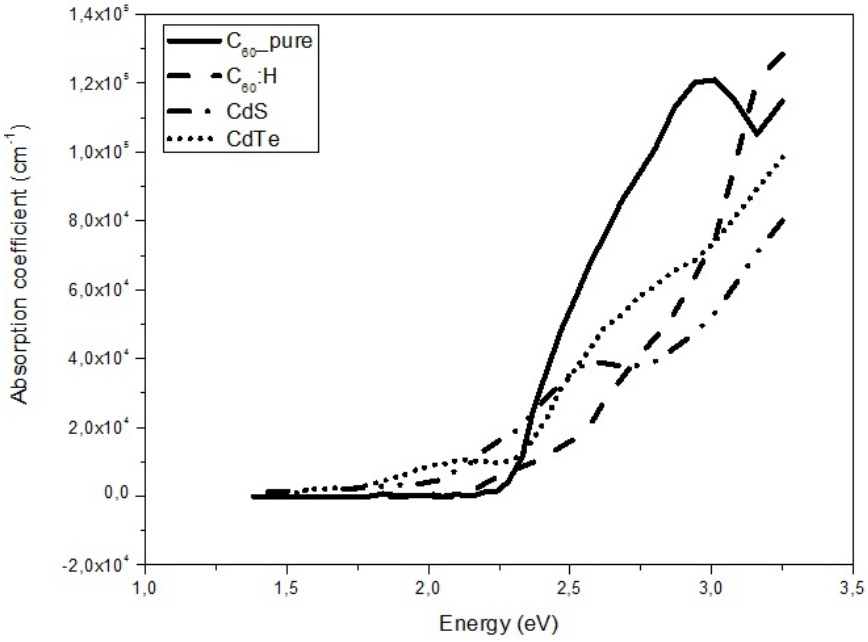

FIG. 6. The absorption coefficients of the films

According to Figure 6, the pristine C_{60} film presents high transparency until 2.2 eV. Above 2.2 eV, a very strong absorption increase was observed, which is probably showing the absorption of excitons. The peak in 2.8 eV can be related to a CT- electron. The CdTe intercalated films gave weak absorbing properties in the 1.5–2 eV region, which may be a result of CdTe itself having an optical threshold at 1.5 eV. There is also one additional mechanism of absorption switch which is present at about 2.2 eV. However, CdS intercalated films displayed more transparency than CdTe films. The optical absorption of CdS films start

approximately at 2.74 eV (4500 Å). Additionally, C_{60}CdS films already begin to absorb at 2 eV, which may possibly be related to the created impurity levels in the molecular C_{60} solids. The hydrogen plasma-treatmed film doesn't provide any prominent absorption features in the investigated spectral range. The absorption features on the film likely depend on the Frenkel excitons and there are no signals related to CT-excitons. As a final result, it is noted that pristine C_{60} film presents the highest absorption in the 2.5–3.5 eV region. The intercalated and plasma treatment films present more transparency. This phenomenon can be explained by the CT-exciton being formed in a pristine C_{60} film, whereas it is suppressed in the intercalated films.

4. Summary and Conclusions

In this project, the CdS, CdTe, HNO_3, TPP-intercalated and hydrogen plasma-treated fullerene films were studied to determine their ability to generate singlet oxygen. As both polymerization and the generation of singlet oxygen require the triplet state of fullerene, we anticipated that mechanical isolation by the molecules such as weak charge transfer properties or dilute hydrogen functionalization can suppress the polymerization. Raman spectroscopy was used to monitor the polymerization process on the films. The $A_g(2)$ mode was found to split in all cases, except for freshly hydrogen plasma-treated films. The splitting in the $A_g(2)$ mode was very strong in HNO_3- and TPP- intercalated films. CdS and CdTe films also presented the features of $A_g(2)$ - derived modes, which were weaker than the pristine C_{60} film. The absorption spectra for pristine C_{60} film had a prominent spectral band linked to CT-excitons. The absorption in the CT-exciton band was much smaller for CdS and CdTe films, whereas it was totally absent in the investigated spectral range for plasma-treated films.

Acknowledgements

The work is supported by the EU FP7 Marie Curie IRSES Project 269138 "Nano-Guard".

References

[1] D. Guldi, M. Prato. Excited-state properties of C_{60} fullerene derivatives. *Accounts of Chemical Research*, **33**, P. 695–703 (2000).

[2] D. M. McCluskey, T. N. Smith, P. K. Madasu, C. E. Coumbe, M. A. Mackey, P. A. Fulmer, J. H. Wynne, S. Stevenson, J. P. Phillips. Evidence for Singlet Oxygen Generation and Biocidal Activity in Photoresponsive Metallic Nitride Fullerene-Polymer Adhesive Films. *ACS Appl. Mater. & Interfaces*, **1**, P. 882–887 (2009).

[3] C. S. Foote. Photophysical and photochemical properties of fullerenes. In: *Electron Transfer I*, ed.J. Mattay, Springer Berlin, Heidelberg, (1994) p. 1-17.

[4] V. V. Zarubaev, I. M. Belousova, O. I. Kiselev, L. B. Piotrovsky, P. M. Anfimov, T. C. Krisko, T. D. Muraviova, V. V. Rylkov, A. M. Starodubzev, A. C. Sirotkin. Photodynamic inactivation of influenza virus with fullerene C_{60} suspension in allontoic fluid. *Photodiagnosis and Photodynamic Therapy*, **4**, P. 31-35 (2007).

[5] F. Käsermann, C. Kempf. Photodynamic inactivation of enveloped viruses by buckmisterfullerene. *Antiviral Research*, **34**, P. 65–70 (1997).

[6] Y. Kai, Y. Komazawa, A. Miyajima, N. Miyata, Y. Yamakoshi. [60] Fullerene as a Novel Photoinduced Antibiotic. In: *Fullerenes, Nanotubes and Carbon Nanostructures*, Taylor & Francis, New York (2003), pp. 79-87.

[7] S. Wang, R. Gao, F. Zhou, M. Selke. Nanomaterials and singlet oxygen photosensitiziers: potential applications in photodynamic therapy. *J. Mater. Chem.*, **14**, P. 487–493 (2004).

[8] P. Mroz, G. P. Tegos, H. Gali, T. Wharton, T. Sarna, M. R. Hamblin. Fullerenes as Photosensitiziers in Photodynamic Therapy. In: *Medicinal Chemistry and Pharmacological Potential of Fullerenes and Carbon Nanotubes*, ed. by F. Cataldo and T. D. Ros, Springer (2008), pp. 79-106.

[9] T. Wågberg. Studies of polymeric and intercalated phases of C_{60}, Umeå University, Umeå (2001).

[10] T. Wågberg, P. Jacobsson, B. Sundqvist. Comparative Raman study of photopolymerized and pressure-polymerized C_{60} films. *Phys. Rev. B*, **60**, P. 4535–4538 (1999).

[11] A. N. Andriotis, M. Menon, R. M. Sheetz, E. Richter. McConnel Model for the Magnetism of C_{60}-based Polymers. In: *Carbon-Based Magnetism: An Overview of the Magnetism of Metal Free Carbon-Based Compounds and Materials*, ed. by T. L. Makarova and F. Palacio. B. V. Elsevier, Amsterdam (2006), pp. 483–500.

[12] A. V. Okotrub, V. V. Belavin, L. G. Bulusheva, V. A. Davydov, T. L. Makarova, D. Tomanek. Electronic structure and properties of rhombohedrally polymerized C_{60}. *J. Chem. Phys.*, **115**, P. 5637–5641 (2001).

[13] M. Yesilbas. *Evaluation of fullerene-based films ability to suppress spontaneous polymerization*, Umeå University, Umeå (2012).

[14] D. Porezag, M. R. Pederson, T. Frauenheim, T. Khler. Structure, stability, and vibrational properties of polymerized C_{60}. *Phys. Rev. B*, **52**, P. 14963–14970 (1995).

[15] T. Wågberg, P.-A. Persson, B. Sundqvist. Structural evolution of low-pressure polymerised C_{60} with polymerisation conditions. *J. Phys. Chem. Solids*, **60**, P. 1989–1994 (1999).

[16] P.C. Elkund. Phototransformation of fullerenes. Patent US5453413 (1993).

[17] A. M. Rao, Zhou Ping, Wang Kai-An et. al. Photoinduced Polymerization of Solid C_{60} Films. *Science*, **259**(5097), P. 955–957 (1993).

[18] Z.-H. Dong, P. Zhou, J. M. Holden, P. C. Eklund, M. S. Dresselhaus, G. Dresselhaus. Observation of higher-order Raman modes in C_{60} films. *Phys. Rev. B*, **48**, P. 2862–2865 (1993).